Articles

Remarkable Influence of X and R on the Charge Transfer Character (MLCT or XLCT) of the Complexes [Ru(X)(R)(CO)$_2$(L)] (X = Halide, CF$_3$SO$_3$; R = Alkyl; L = α-Diimine): A UV–Vis Absorption and Resonance Raman Study

Heleen A. Nieuwenhuis, Derk J. Stufkens,[*] and Ad Oskam

Anorganisch Chemisch Laboratorium, Universiteit van Amsterdam,
Nieuwe Achtergracht 166, 1018 WV Amsterdam, The Netherlands

Complexes of the type [Ru(X)(R)(CO)$_2$(L)] (X = halide, CF$_3$SO$_3$; R = alkyl; L = N,N'-diisopropyl-1,4-diaza-1,3-butadiene, pyridine-2-carbaldehyde N-isopropylimine, 2,2'-bipyridine) experience significant influences of X and R on the energies and relative intensities of their lowest-energy electronic transitions. The halide complexes show two absorption bands in the visible region, which are assigned to two sets of charge transfer transitions from mixed metal–halide orbitals. Variation of the halide from Cl to I gives rise to a change in character of the lowest-energy band from MLCT to XLCT, as evidenced by resonance Raman spectra. These spectra show enhancement of Raman intensity for both ν_s(CN) and ν_s(CO) in the case of the Cl complex, but only for ν_s(CN) for the corresponding I complex. Variation of the alkyl ligand from Me to iPr leads to a shift of both absorption bands to lower energy with a concomitant change of their relative intensities. The latter effect is again ascribed to a change of charge transfer character of the electronic transitions.

Introduction

Many transition metal complexes having a lowest metal-to-ligand charge transfer (MLCT) state can undergo efficient energy and electron transfer processes. Best known in this respect are the complexes [Ru(bpy)$_3$]$^{2+}$ [1–5] and [Re(L)(CO)$_3$(bpy)] (L = halide, N-donor ligand).[6–13] Both types of compounds are emissive, but the excited states of the Ru^{II} complexes are usually longer lived than those of similar Re^I complexes. Apart from the higher photostability, a great advantage of the Re^I complexes above the Ru^{II} species is that their excited state properties can strongly be influenced by variation of L.[14–17] Thus, ligands such as 4,4'-bipyridine[18,19] and CN$^-$ [20] can act as an efficient bridge to other metal fragments and, for L being an organic donor[21,22] (e.g.

4-dimethylaminobenzonitrile) or acceptor[23] (e.g. N-methyl-4,4'-bipyridinium cation), chromophore–quencher complexes are formed, which show interesting intramolecular electron transfer reactions.

In order to increase the versatility of the ruthenium compounds, we have synthesized a series of [Ru(X)(R)(CO)$_2$(α-diimine)] complexes, for which the ligand field is stronger than for [Ru(bpy)$_3$]$^{2+}$ and in which the ligands X and R can easily be varied. Two other reasons led to the selection of these complexes for detailed spectroscopic, photophysical and photochemical study. Recently, it has been established by our group that the highest-filled molecular orbitals of the complexes [M(X)(CO)$_3$(α-diimine)] (M = Mn, Re; X = halide) have strongly mixed metal–halide character.[24,25] Similar behavior was expected for these Ru–halide complexes and therefore special attention was paid to the influence of X and R on the electronic properties. Another interesting aspect of these complexes is the presence of an alkyl group. In case of the closely related compounds [Re(R)(CO)$_3$(R'-DAB)] (R, R' = alkyl) variation of R has recently been shown to influence strongly their photoreactivity.[26] Similar behavior might be expected for these Ru compounds.

In this article we describe the spectroscopic properties (UV–vis, resonance Raman) of these [Ru(X)(R)(CO)$_2$(α-diimine)] complexes, with special attention paid to the influence of X and R. The photophysical and photochemical properties will be reported in forthcoming articles.

The syntheses and molecular structures of several of these complexes have been first described by tom Dieck and co-workers.[27,28] The complexes have a distorted octahedral conformation with two CO ligands in the equatorial plane of the

* To whom correspondence should be addressed.
⊛ Abstract published in *Advance ACS Abstracts*, June 15, 1994.
(1) Juris, A.; Balzani, V. *Coord. Chem. Rev.* **1988**, *84*, 85.
(2) Kalyanasundaram, K. *Coord. Chem. Rev.* **1982**, *46*, 159.
(3) Meyer, T. J. *Pure Appl. Chem.* **1986**, *58*, 1193.
(4) Krausz, E.; Ferguson, J. *Prog. Inorg. Chem.* **1989**, *37*, 293.
(5) Watts, R. J. *J. Chem. Educ.* **1983**, *60*, 834.
(6) Stufkens, D. J. *Comments Inorg. Chem.* **1992**, *13*, 359.
(7) Wrighton, M.; Morse, D. L. *J. Am. Chem. Soc.* **1974**, *96*, 998.
(8) Geoffroy, G. L.; Wrighton, M. In *Organometallic Photochemistry*; Academic Press: New York, 1979.
(9) Juris, A.; Campagna, S.; Bidd, I.; Lehn. J.-M.; Ziessel, R. *Inorg. Chem.* **1988**, *27*, 4007.
(10) Kaim, W.; Kramer, H. E. A.; Vogler, C.; Rieker, J. *J. Organomet. Chem.* **1989**, *367*, 107.
(11) Kalyanasundaram, K. *J. Chem. Soc., Faraday Trans. 2* **1986**, *82*, 2401.
(12) Sullivan, P. *J. Phys. Chem.* **1989**, *93*, 24.
(13) Worl, L. A.; Duesing, R.; Chen, P.; Della Ciana, L.; Meyer, T. J. *J. Chem. Soc. Dalton Trans.* **1991**, 849.
(14) Baiano, J. A.; Murphy, Jr., W. R. *Inorg. Chem.* **1991**, *30*, 4594.
(15) Sacksteder, L.; Zipp, A. P.; Brown, E. A.; Streich, J.; Demas, J. N.; DeGraff, B. A. *Inorg. Chem.* **1990**, *29*, 4335.
(16) Hino, J. K.; Della Ciana, L.; Dressick, W. J.; Sullivan, B. P. *Inorg. Chem.* **1992**, *31*, 1072.
(17) Caspar, J. V.; Meyer, T. J. *J. Phys. Chem.* **1983**, *87*, 952.
(18) Tapolsky, G.; Duesing, R.; Meyer, T. J. *J. Phys. Chem.* **1989**, *93*, 3885.
(19) Tapolsky, G.; Duesing, R.; Meyer, T. J. *Inorg. Chem.* **1990**, *29*, 2285.
(20) Lin, R.; Guarr, T. F. *Inorg. Chim. Acta* **1990**, *167*, 149.
(21) Perkins, T. A; Humer, W.; Netzel, T. L.; Schanze, K. S. *J. Phys. Chem.* **1990**, *94*, 2229.
(22) MacQueen, D. B.; Schanze, K. S. *J. Am. Chem. Soc.* **1991**, *113*, 7470.
(23) Chen, P.; Danielson, E.; Meyer, T. J. *J. Phys. Chem.* **1988**, *92*, 3708.
(24) Stor, G. J.; Stufkens, D. J.; Vernooijs, P.; Baerends, E. J.; Fraanje, J.; Goubitz, K. *Inorg. Chem.*, in press.
(25) Stor, G. J.; Stufkens, D. J.; Oskam, A. *Inorg. Chem.* **1992**, *31*, 1318.
(26) Rossenaar, B. D.; Kleverlaan, C. J.; Stufkens, D. J.; Oskam, A. *J. Chem. Soc., Chem. Commun.* **1994**, 63.
(27) Rohde, W.; tom Dieck, H. *J. Organomet. Chem.* **1987**, *328*, 209.
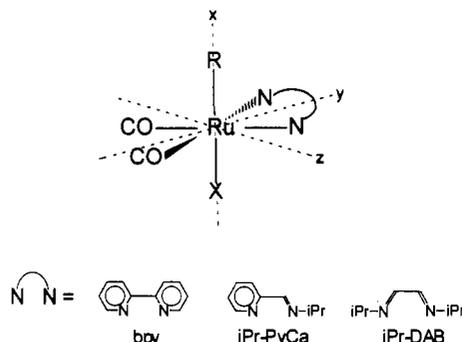
Figure 1. Schematic structures of $[Ru(X)(R)(CO)_2(\alpha\text{-diimine})]$ and the α-diimines bpy, iPr-PyCa, and iPr-DAB.

α-diimine ligand and the alkyl and halide in axial positions. Figure 1 presents the schematic structure of the complexes and α-diimine ligands used (X = halide, CF_3SO_3; R = alkyl; α-diimine = 2,2'-bipyridine (bpy), pyridine-2-carbaldehyde N-isopropylimine (iPr-PyCa), N,N'-diisopropyl-1,4-diaza-1,3-butadiene (iPr-DAB)). The complexes $[Ru(X)(R)(CO)_2(\alpha\text{-diimine})]$ will further be denoted as X/R/α-diimine, which means that e.g. I/Me/iPr-DAB stands for the complex $[Ru(I)(Me)(CO)_2(iPr\text{-DAB})]$.

Experimental Section

Materials and Preparations. $[Ru_3(CO)_{12}]$, bpy, MeI, EtI, and iPrI were purchased and used without further purification. Solvents for synthetic purposes were of reagent grade, dried on sodium wire (THF, hexane) or $CaCl_2$ (CH_2Cl_2), and freshly distilled under N_2 atmosphere before use. For UV–vis and resonance Raman measurements solvents of spectroscopic grade were used.

The ligands N,N'-diisopropyl-1,4-diaza-1,3-butadiene (iPr-DAB) and pyridine-2-carbaldehyde N-isopropylimine (iPr-PyCa) were synthesized by literature methods.[29] The complexes $[Ru(X)(Me)(CO)_2(iPr\text{-DAB})]$ (X = I, CF_3SO_3) and $[Ru(I)(Me)(CO)_2(iPr\text{-PyCa})]$ were prepared according to literature methods.[30]

$[Ru(X)(R)(CO)_2(iPr\text{-DAB})]$ (X, R = I, Et; Br, Et; I, iPr) complexes were prepared by a modified literature method.[30] A 1-mmol sample of $[Ru_3(CO)_{12}]$, 3.1 mmol of iPr-DAB and a 10-fold excess of R–X were dissolved in 50 mL of hexane and refluxed for 2.5 h under nitrogen atmosphere. After evaporation to dryness under vacuum the compounds were purified by column chromatography over silica and recrystallized from THF/hexane at –30 °C.

I/Et/iPr-DAB: Yield: 48%. IR (THF): 2022, 1958 cm⁻¹. ¹H-NMR (CDCl₃): δ 8.11 (s) (2 imine-CH), 4.50 (m) (2 iPr-CH), 1.56 (d) (12 iPr-CH₃), 1.34 (t) (3 Et-CH₃), 0.89 (m) (2 Et-CH₂). Anal. Found (calcd for C₁₂H₂₁IN₂O₂Ru): C, 31.72 (31.79); H, 4.57 (4.64); N, 6.16 (6.18).

Br/Et/iPr-DAB: Yield: 53%. IR (THF): 2022, 1955 cm⁻¹. ¹H-NMR (CDCl₃): δ 8.21 (s) (2 imine-CH), 4.39 (m) (2 iPr-CH), 1.55 (d) (12 iPr-CH₃), 1.29 (t) (3 Et-CH₃), 0.89 (m) (2 Et-CH₂). Anal. Found (calcd for C₁₂H₂₁BrN₂O₂Ru): C, 35.73 (35.47); H, 5.19 (5.17); N 6.76 (6.90).

I/ iPr/ iPr-DAB: Yield: 31%. IR (THF): 2022, 1959 cm⁻¹. ¹H-NMR (CDCl₃): δ 8.24 (s) (2 imine-CH), 4.54 (m) (2 iPr-CH), 1.61 (d) (6 iPr-CH₃), 1.49 (d) (6 iPr-CH₃), 1.20 (d) (6 iPr-CH₃) 1.34 (t), 0.04 (m) (1 iPr-CH₂). Anal. Found (calcd for C₁₃H₂₃IN₂O₂Ru): C, 33.28 (33.41); H, 4.99 (4.96); N, 5.94 (5.99).

$[Ru(X)(Me)(CO)_2(iPr\text{-DAB})]$ (X =Cl, Br) was synthesized according to literature methods.[31] $[Ru(CF_3SO_3)(Me)(CO)_2(iPr\text{-DAB})]$ was dissolved in dichloromethane and stirred for 2 h with excess $(Et)_4NCl$ and $(tBu)_4NBr$, respectively. The products were purified by column chromatography over silica and recrystallized from THF/hexane.

Cl/Me/iPr-DAB: Yield: 95%. IR (THF): 2024, 1955 cm⁻¹. ¹H NMR (CDCl₃): δ 8.20 (s) (2 imine-CH), 4.32 (m) (2 iPr-CH), 1.41

(2*d) (12 iPr-CH₃), –0.22 (s) (3 CH₃). Anal. Found (calcd for C₁₁H₁₉ClN₂O₂Ru): C, 37.92 (37.99); H, 5.45 (5.47); N, 7.94 (8.06).

Br/Me/iPr-DAB: Yield: 95%. IR (THF): 2023, 1956 cm⁻¹. ¹H-NMR (CDCl₃): δ 8.16 (s) (2 imine-CH), 4.36 (m) (2 iPr-CH), 1.55 (2 *d) (12 iPr-CH₃), –0.17 (s) (3 CH₃). Anal. Found (calcd for C₁₁H₁₉BrN₂O₂Ru): C, 33.59 (33.67); H, 4.95 (4.85); N, 7.04 (7.14).

For the synthesis of $[Ru(I)(Me)(CO)_2(bpy)]$ a modified literature method was used,[32] which started with the preparation of $[Ru(I)_2(CO)_2\text{-}(bpy)]$ by stirring 1 mmol of $[Ru(I)_2(CO)_2(MeCN)_2]$[33] and 1.1 mmol of bpy at 70 °C in toluene for 0.5 h. The solvent was evaporated under vacuum, and the compound was purified by washing with hexane to remove excess bpy. It was then dissolved in dichloromethane for column purification (silica gel; eluent dichloromethane). 1 mMol $[Ru(I)_2(CO)_2\text{-}(bpy)]$ was then dissolved in 50 mL of THF under N_2 and reduced by excess $Na_{2.1}K$ for 2 h. After filtration of the excess NaK, 0.5 mL of MeI was added to the filtrate, and the mixture was stirred and refluxed for half an hour. After evaporation of the solvent the complex $[Ru(I)(Me)\text{-}(CO)_2(bpy)]$ was purified by column chromatography over silica and recrystallized from THF/hexane.

I/I/bpy: Yield: 68%. IR (THF): 2050, 1993 cm⁻¹. UV–vis (THF): 399 (ε = 1580 dm³ mol⁻¹ cm⁻¹), 310 (ε = 11 000 dm³ mol⁻¹ cm⁻¹) nm. ¹H-NMR (CDCl₃): δ 9.13 (d) (2 bpy-H3), 8.17 (t) (2 bpy-H4), 8.06 (d) (2 bpy-H6), 7.59 (2 bpy-H5). Anal. Found (calcd for C₁₂H₈I₂N₂O₂-Ru): C, 25.32 (25.40); H, 1.47 (1.41); N, 4.98 (4.94).

I/Me/bpy: Yield: 10–40%. IR (THF): 2023, 1956 cm⁻¹. ¹H NMR: δ 8.98 (d) (2 bpy-H3), 8.14 (t) (2 bpy-H4), 7.94 (d) (2 bpy-H6), 7.52 (2 bpy-H5), 0.08 (s) (3 CH₃). Anal. Found (calcd for C₁₃H₁₁IN₂O₂-Ru): C, 34.51 (34.29); H, 2.99 (2.42); N, 5.73 (6.15).

Spectroscopic Measurements. Electronic absorption spectra were recorded on a Perkin-Elmer Lambda 5 UV/vis spectrophotometer, equipped with a Model 3600 data station, and on a Varian Cary 04e spectrophotometer. Resonance Raman measurements were performed on a Dilor XY spectrometer, using a SP Model 2016 argon ion laser as the excitation source. IR spectra were measured on a Nicolet 7199 B FTIR spectrophotometer with a liquid-nitrogen-cooled MCT detector, or a BioRad FTS-7 FTIR spectrometer. ¹H-NMR spectra were recorded on a Bruker AC100 or a AMX300 spectrometer. Elemental analyses were carried out by the Microanalytisches Laboratorium of Dornis und Kolbe, Mülheim a. d. Ruhr, Germany.

Results

Syntheses. Tom Dieck and co-workers were the first who described a synthesis route for these complexes, in which the complex X/X/R-DAB was first reduced and an alkyl-halide RX was allowed to react with the reduced species producing the complex X/R/R-DAB.[27,28] Because of the complexity of this procedure, another route was used, which has first been described by Kraakman et al.[30] According to this procedure $[Ru_3(CO)_{12}]$, iPr-DAB, and MeI were refluxed in heptane or hexane and the complex I/Me/iPr-DAB precipitated from the solution. This procedure could also be applied for other alkyl halide–α-diimine complexes, with the exception of the bpy compound. In the latter case formation of the stable complex $[Ru_3(CO)_{10}(bpy)]$ prevented the formation of the desired product. For the preparation of these bpy-complexes the tom Dieck method was employed. The complexes are air stable and, with exception of the complexes I/iPr/iPr-DAB, I/Me/bpy, and I/Me/iPr-PyCa, they are also photostable.

Electronic Absorption Spectra. The absorption characteristics of the complexes are collected in Table 1. Figure 2a presents the spectra of the three representative complexes X/Me/iPr-DAB (X = Cl, Br, I) and Figure 2b those of X/Me/iPr-DAB (X = CF_3SO_3, I) in the wavelength region 300–700 nm.

The spectrum of the chloride complex shows a weak shoulder at about 330 nm and a band at 435 nm. The shoulder is more pronounced in the spectrum of the bromide complex and becomes a strong band for the corresponding iodide complex. In fact,

(28) tom Dieck, H.; Rohde, W.; Behrens, U. *Z. Naturforsch.* **2 1989**, *44B*, 158.
(29) Bock, H.; tom Dieck, H. *Chem. Ber.* **1967**, *100*, 228.
(30) Kraakman, M. J. A.; Vrieze, K.; Kooijman, H.; Spek, A. L. *Organometallics* **1992**, *11*, 3760.
(31) Servaas, P. C.; Stufkens, D. J.; Oskam, A.; Vernooijs, P.; Baerends, E. J.; De Ridder, D. J. A.; Stam, C. H. *Inorg. Chem.* **1989**, *28*, 4104.

(32) tom Dieck, H.; Kollvitz, W.; Kleinwächter, I.; Rohde, W.; Stamp, L. *Transition Met. Chem. (Weinheim, Ger.)* **1986**, *11*, 361–366.
(33) Irving, R. J. *J. Chem. Soc.* **1956**, 2879.

Table 1. UV–Vis Spectral Data for [Ru(X)(R)(CO)$_2$(α-diimine)] in THF at Room Temperature (λ_{max} in nm; ϵ in M^{-1} cm^{-1})

α-diimine	R	X	$\lambda_{max}(1)$ (ϵ)	$\lambda_{max}(2)$ (ϵ)	$\lambda_{max}(3)$ (ϵ)
iPr-DAB	Me	I	463 (1555)	374 (2630)	298 (3200)
iPr-DAB	Me	Br	449 (1640)	334 (sh) (1780)	292 (2740)
iPr-DAB	Me	Cl	435 (1710)	~330 nm (sh) (~1100)	280 (2310)
iPr-DAB	Me	CF$_3$SO$_3$	380 (2180)		
iPr-DAB	Et	I	453 (1700)	397 (2100)	
iPr-DAB	iPr	I	479 (2120)	428 (1890)	
iPr-PyCa	Me	I	427 (1970)	350 (2810)	
bpy	Me	I	403 (1800)		
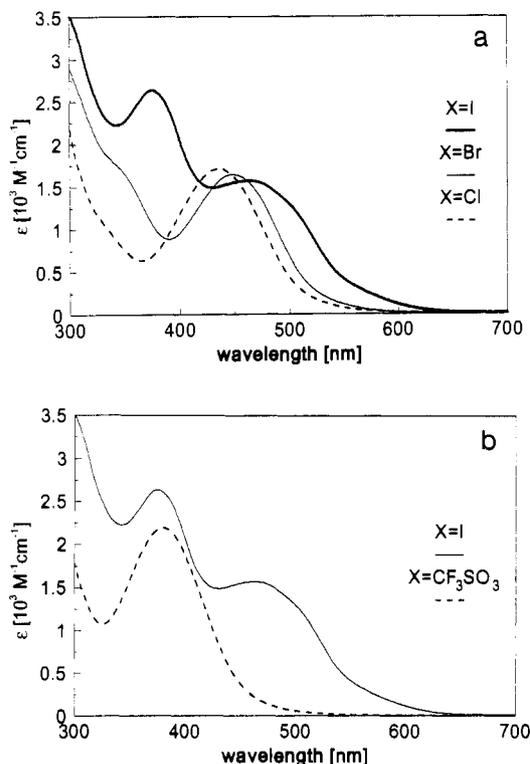
Figure 2. Absorption spectra of [Ru(X)(Me)(CO)$_2$(iPr-DAB)] in THF at room temperature: (a) X = Cl, Br, I; (b) X = I, CF$_3$SO$_3$.

Figure 3. Absorption spectra of [Ru(I)(R)(CO)$_2$(iPr-DAB)] (R = Me, Et, iPr) in THF at room temperature.

Figure 4. Absorption spectra of [Ru(I)(Me)(CO)$_2$(α-diimine)] (α-diimine = bpy, iPr-PyCa, iPr-DAB) in THF at room temperature.

Table 2. Solvatochromism of the Absorption Bands of [Ru(X)(Me)(CO)$_2$(iPr-DAB)] (X = Cl, I) at Room Temperature

solvent	$\lambda_{max,abs}$(Cl/Me/iPr-DAB)[a]	$\lambda_{max,abs}$(I/Me/iPr-DAB)[a]
acetonitrile	416, 279	436, 360, 293
acetone	424	443, 365
tetrahydrofuran	435, 280	463, 374, 298
toluene	451	485, 386, 295

[a] In nm.

variation of the halide from Cl to I has two different effects on the first two absorption bands. Both absorptions, the shoulder and the lowest-energy band, shift to longer wavelengths. Simultaneously, a drastic change in the relative intensities of these two bands is observed. Whereas the extinction coefficients of the lowest-energy bands of the three complexes are comparable (1550–1750 M^{-1} cm^{-1}), the second absorption becomes much stronger going from the Cl to the I complex (ϵ_{max} = ca. 1100–2600 M^{-1} cm^{-1}). Contrary to the halide complexes, the CF$_3$SO$_3$ compound (Figure 2b) shows only one low-energy absorption band with ϵ_{max} = 2180 M^{-1} cm^{-1}.

Figure 3 clearly shows that variation of the alkyl group has also a large influence on the positions and relative intensities of the two absorption bands in case of the I/R/iPr-DAB complexes. Going from R = Me to the more electron releasing iPr-ligand, both absorption bands shift to lower energy. At the same time the intensity of the first absorption band increases at the expense of that of the second band (Table 1 and Figure 3). The spectrum of the ethyl complex shows an intermediate intensity pattern for these two absorption bands.

Varying the α-diimine ligand from iPr-DAB to iPr-PyCa and bpy causes a shift of both absorption bands to higher energy (Figure 4). The shifts are closely related to the changes in energy of the lowest π^*-orbital of the α-diimine ligand.[34] In case of the bpy ligand the shifts are so large, that the second absorption band

has disappeared completely under the much stronger absorptions at shorter wavelengths.

The influence of the polarity of the solvent on the positions of the absorption bands has been studied for the complexes Cl/Me/iPr-DAB and I/Me/iPr-DAB. The results are collected in Table 2. The lowest-energy bands of I/Me/iPr-DAB show large shifts to the red of 2320 and 1870 cm^{-1}, respectively, going from MeCN to toluene. For the Cl/Me/iPr-DAB complex a solvent dependent shift of 1870 cm^{-1} is observed. The third band of I/Me/iPr-DAB, at about 300 nm, only shows a minor shift (230 cm^{-1}), going from MeCN to toluene, which even does not agree with the change in polarity of the solvent.

Resonance Raman Spectra. Resonance Raman (rR) spectroscopy has proven to be a very valuable technique for the assignment of allowed electronic transitions.[35,36] Since only those vibrations will be resonance enhanced that are vibronically coupled to the electronic transitions, these transitions can be characterized by the observed resonance effects. Resonance Raman spectra were recorded for the complexes under study, with exciting laser lines ranging from 457.9 to 514.5 nm. The spectra of the photostable complexes were measured from solutions in dichloromethane. Those of the photoreactive bpy-complex were recorded in a KNO$_3$ disk. The main Raman bands, which are

(34) Reinhold, J; Benedix, R; Birner, P; Hennig, H. *Inorg. Chim. Acta* **1979**, *33*, 209.

(35) Balk, R. W.; Snoeck, T.; Stufkens, D. J.; Oskam, A. *Inorg. Chem.* **1980**, *19*, 3015.

(36) Balk, R. W.; Stufkens, D. J.; Oskam, A. *J. Chem. Soc., Dalton Trans.* **1981**, 1124.

Table 3. Resonance-Enhanced Raman Bands (Wavenumbers in cm⁻¹) for [Ru(XO)(R)(CO)2(α-diimine)] Complexes Measured in CH2Cl2 (Unless Stated Otherwise)

X/R/α-diimine	Raman wavenumbers, cm⁻¹
I/Me/iPr-DAB	2033, 1555, 1293, 1201, 1057, 501, 481, 419, 169
Br/Me/iPr-DAB	2037, 1561, 1206, 1053, 485, 424, 186
Cl/Me/iPr-DAB	2033, 1568, 1212, 487, 421, 183
CF3SO3/Me/iPr-DAB	2034, 1571, 1217, 512, 485, 191
I/Et/iPr-DAB	2033, 1548, 1293, 1027, 485, 140
I/Me/iPr-PyCa	1618, 1560, 1514, 1478, 1304, 1256, 1240, 1204, 1025, 604, 591, 512, 492, 138
I/Me/bpy[a]	1603, 1562, 1491, 1358, 1345, 1314, 1283, 1202, 1168, 1031, 715, 509, 491, 197, 126

[a] In KNO3 disk.
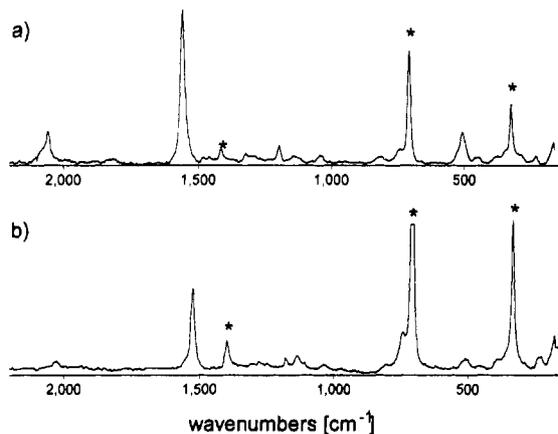
Figure 5. Raman spectra of (a) [Ru(Cl)(Me)(CO)2(iPr-DAB)] (λ_{exc} = 476.9 nm) and (b) [Ru(I)(Me)(CO)2(iPr-DAB)] (λ_{exc} = 488.0 nm) in CH2Cl2 at room temperature.

resonance enhanced, are collected in Table 3. Figure 5 presents the Raman spectra of two different complexes, I/Me/iPr-DAB and Cl/Me/iPr-DAB.   t

The Raman bands can be assigned by comparison with literature data on the closely related complexes [M(CO)4(α-diimine)] (M = Cr, Mo, W)[35] and [Re(X)(CO)3(α-diimine)].[36] The spectra of the iPr-DAB complexes only show one strong band in the ligand stretching region at about 1560 cm⁻¹, which belongs to ν_s(CN), the symmetrical stretching mode of the imine groups. The position of this band depends on the metal and the coligands and occurs at 1500 cm⁻¹ for the corresponding [M(CO)4(iPr-DAB)] (M = Cr, Mo, W) complexes. For the corresponding iPr-PyCa and bpy complexes more Raman bands are observed in the frequency region 1400–1700 cm⁻¹, which all belong to symmetrical stretching modes of the imine group and/or pyridine ring.

All complexes show only a weak or very weak rR effect for ν_s(CO) at ca. 2030 cm⁻¹ upon excitation at 514.5 nm. In agreement with expectations and with the results from similar Raman investigations of transition metal α-diimine carbonyls,[35,36] the corresponding asymmetric CO vibration is only observed in the IR spectra, at 1960 cm⁻¹. When the excitation wavelength is changed to 458 nm, the resonance Raman effect of ν_s(CO) increases for nearly all complexes.

A very remarkable difference in behavior is observed for ν_s-(CO) of the complexes Cl/Me/iPr-DAB and I/Me/iPr-DAB. The Cl complex shows a gradual increase of intensity for both the ν_s(CN) and ν_s(CO) Raman bands upon going to shorter wavelengths of excitation. On the other hand, excitation into the first transition of the I complex only gives rise to resonance enhancement of ν_s(CN). This is clearly demonstrated by the rR excitation profiles of these vibrations, depicted for the two complexes in Figure 6. The implications of these results will be discussed in the next section.

The assignment of the low-frequency Raman bands is not straightforward, since several metal-ligand stretching and bending
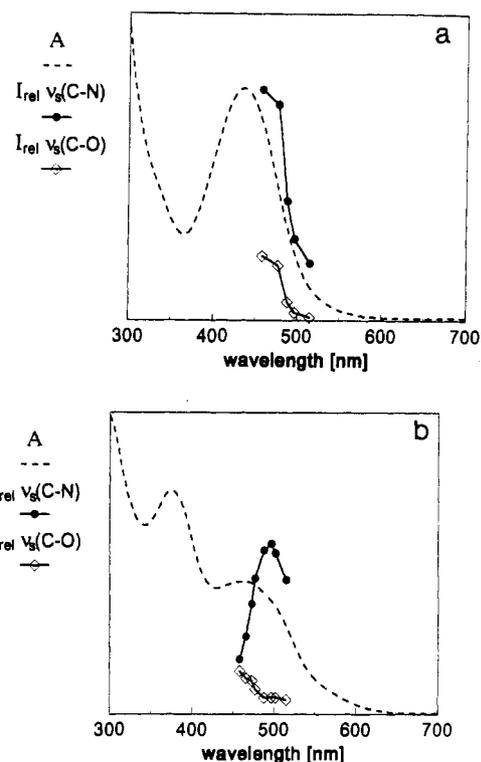
Figure 6. RR excitation profiles for ν_s(CN) and ν_s(CO) of (a) [Ru-(Cl)(Me)(CO)2(iPr-DAB)] and (b) [Ru(I)(Me)(CO)2(iPr-DAB)]. The intensities (I_{rel}) of ν_s(CN) and ν_s(CO) were measured relative to the intensity of the 708-cm⁻¹ band of CH2Cl2.

modes and ligand deformations are close in frequency. The following literature data are of importance here. The IR spectra of the complexes [CsRu(CO)3I3] show ν(Ru–X) at 320 and 285 cm⁻¹ for X = Cl, at 235 cm⁻¹ for X = Br, and at 194 and 177 cm⁻¹ for X = I.[37] For the complex [Ru(CH3)(X)(PP)] (X = halide, PP = (Me)2P(CH2)2P(Me)2), ν(Ru–C) is found at 483 and 465 cm⁻¹ for X = Cl and I, respectively.[38] The Ru–C–O deformation modes of cis-[Ru(Cl)2(CO)2(PEt3)2] have been found at 584 and 498 cm⁻¹.[39] The Raman data of the complexes under study cannot be compared with those of [Ru(CO)3(iPr-DAB)],[40] because of the different charges of the central metals.

Discussion

The absorption spectra of the various X/R/α-diimine complexes, depicted in Figures 2–4, show that the positions of the first two bands strongly depend on the α-diimine ligand, X, and R. A shift to lower energy occurs when bpy is replaced by an α-diimine ligand that has its π^*-orbital at lower energy, such as iPr-PyCa or iPr-DAB (Figure 4). On the basis of these effects, the bands are assigned to charge transfer transitions to the α-diimine ligand. This assignment is confirmed by the rather large intensities of the bands, by their solvent dependencies (Table 2) and by the rR spectra, obtained by excitation into these bands (Figure 5). The latter spectra show resonance enhancement of Raman intensity for the symmetrical stretching modes of the α-diimine ligand, which proves that the electronic transitions involved are indeed directed toward this ligand.

The two well-separated bands might in principle belong to MLCT transitions from different metal-d_π orbitals to the lowest π^* orbital of the α-diimine or be directed to different π^* orbitals of this ligand. Both assignments are, however, not correct. The

(37) Cleare, M. J.; Griffith, W. P. *J. Chem. Soc. A* **1969**, 372.
(38) Chatt, J.; Hayter, R. G. *J. Chem. Soc.* **1963**, 6017.
(39) Adams, D. M. In *Metal–Ligand and Related Vibrations;* Edward Arnold Publishers Ltd: London, 1967, p 128.
(40) Balk, R. W.; Stufkens, D. J.; Oskam, A. *J. Chem. Soc., Dalton Trans.* **1982**, 275.
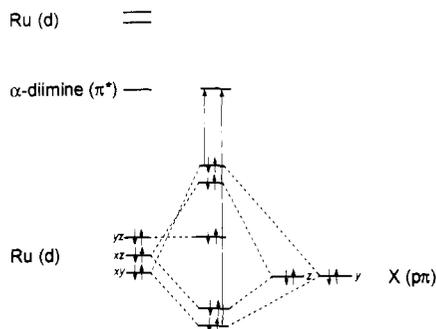
Figure 7. Qualitative MO scheme of [Ru(X)(R)(CO)$_2$(α-diimine)].

former transitions are always close in energy and only give rise to a single composite bands as, e.g., in the case of the [M(CO)$_4$-(α-diimine)] (M = Cr, W, Mo) complexes.[35,41] In view of the occurrence of a single CT band in the visible spectra of these complexes, the second band of the halide complexes under study can also not be assigned to transitions to the second π^* orbital of the α-diimine. The assignment of the two bands to MLCT transitions can also not account for the changes in relative ntensities upon variation of X and R. Finally, this assignment does not agree with the remarkable observation in the rR spectra that the lowest-energy transition of the Cl/Me/iPr-DAB complex affects both the imine and CO bonds, whereas for I/Me/iPr-DAB only the imine bonds are influenced by this transition.

These data can only be explained with a strong mixing between the metal-dπ and halide-pπ orbitals, so that the highest filled orbitals, from which the CT transitions originate, obtain varying metal–halide character, depending on X and R. The schematic MO diagram of Figure 7 shows that the filled d$_{xy}$(Ru) and p$_y$(X) orbitals interact, giving rise to a bonding and antibonding combination. The same holds for the d$_{xz}$(Ru) and p$_z$(X) orbitals. In this way two sets of two orbitals having mixed metal–halide character are obtained, from which the CT transitions originate. The transitions from these sets of orbitals result in the two separate absorption bands. The electronic transition from the pure metal orbital d$_{yz}$(Ru) to the α-diimine is overlap forbidden and will not contribute to the intensities of the two absorption bands.

The lowest-energy band will belong to CT transitions from the antibonding d$_{xy}$(Ru)–p$_y$(X) and d$_{xz}$(Ru)–p$_z$(X) orbitals to the lowest π^* orbital of the α-diimine. The former transition will be more intense, since only d$_{xy}$(Ru) and not d$_{xz}$(Ru) strongly interacts with the π^* orbital (π-back-bonding). Moreover, since p$_y$(X) will have a smaller overlap with the π^* orbital than d$_{xy}$(Ru), the intensity of the y-polarized d$_{xy}$(Ru)–p$_y$(X) $\rightarrow$ π^* (α-diimine) transition will mainly be determined by the contribution of d$_{xy}$-(Ru) to this antibonding combination.

The same reasoning holds for the CT transitions of the second absorption band, which originate from the set of metal–halide bonding orbitals. Thus, the CT transition from the d$_{xy}$(Ru) + p$_y$(X) orbital will be stronger than the transition originating from the d$_{xz}$(Ru) + p$_z$(X) combination. Again, its intensity will mainly be determined by the contribution of d$_{xy}$(Ru) to this molecular orbital.

The formation of these two sets of orbitals explains why the absorption spectra of these complexes differ from those of e.g. CF$_3$SO$_3$/Me/iPr-DAB and [M(CO)$_4$(α-diimine)],[35,41] which only show a single, composite CT band at low energy. In two ways the compositions and relative positions of the highest-filled orbitals can be affected. Either the halide-pπ orbitals are varied in energy by replacing Cl by Br and I, or the positions of the metal-dπ orbitals are influenced by changing the electron-releasing properties of the alkyl ligand. The results of these variations will now be discussed in more detail.

Going from X = Cl to Br and I, the ionization potentials of the halide-pπ orbitals decrease, which was clearly shown by UV-PES measurements on the complexes [M(X)(CO)$_5$] (M = Mn, Re; X = Cl, Br, I).[42] In this way the metal–halide bonding orbitals obtain more metal character, whereas the halide orbitals contribute more to the set of antibonding orbitals. As a result, the transitions from the bonding orbitals become stronger, since they have more MLCT (especially d$_{xy}$(Ru) to π^*) character. Those from the antibonding combination become weaker, since their character gradually changes from MLCT into XLCT upon going from Cl to I. Replacement of the halide ligand by a weakly, and purely σ-bonding ligand such as CF$_3$SO$_3^-$, shows that indeed no mixing occurs between this ligand and the metal-dπ orbitals. Only one absorption band remains, just as for the corresponding [M(CO)$_4$(α-diimine)] (M = Cr, Mo, W) complexes. The position of this band shows that the interaction between the metal-dπ and the halide-pπ orbitals does not only give rise to the presence of two separate absorption bands, but also to a shift of these bands to lower energy.

This change of CT character is confirmed by the rR data obtained by excitation into the first electronic transitions of the X/Me/iPr-DAB (X = Cl, I) complexes. The excitation profiles of Figure 6, in which these rR data are collected, exhibit a rR effect for both ν_s(CN) and ν_s(CO) in case of the Cl complex. For the I complex only enhancement of ν_s(CN) is found. The results for the Cl complex agree with those of many other α-diimine carbonyls, such as [M(CO)$_4$(α-diimine)] (M = Cr, W, Mo)[35] and [Ni(CO)$_2$(α-diimine)].[43] All these complexes show that an increase of MLCT character is accompanied by a concomitant increase of Raman intensity for symmetrical stretching modes of both the α-diimine and the carbonyls. The rR effect of ν_s(CN) is caused by the change of imine bond lengths upon occupation of the π^* orbital, that of the carbonyl stretching mode is due to the decrease of π-backbonding to the carbonyls upon oxidation of the metal. The occurrence of a rR effect for ν_s(CN) and not for ν_s(CO), in case of the I complex, is exceptional. The only reasonable explanation is that electron transfer to the α-diimine does not originate from the metal, but from the halide. This conclusion again confirms that, as mentioned above, changes in character of the lowest-energy transitions occur. A similar low-energy XLCT transition has recently been observed for [Re-(Br)(CO)$_3$(pTol-DAB)], in which case the Raman spectra showed a strong rR effect for ν(Re-Br).[25] Because of this, the low frequency region of the rR spectrum of the I/Me/iPr-DAB complex was also examined more closely. Although these spectra did show a band at 190 cm^{-1}, close to the literature value for ν(Ru–I), this band was also found for the corresponding Cl and Br complexes. It probably belongs to ν_s(Ru–N). Maybe that the Ru–I bond is less influenced by the CT transitions, since the highest-filled orbitals have more halide character than those of [Re(Br)(CO)$_3$(pTol-DAB)].

Interestingly not only the halide but also the alkyl group of these ruthenium complexes can be varied. The alkyl group does not mix with the metal-dπ and halide-pπ orbitals, because of the difference in symmetry between these metal-dπ, halide-pπ, and alkyl-σ orbitals. Therefore, the alkyl ligand will not contribute to the HOMO but variation of R will only have a large influence on the electron density at the metal center. Going from R = Me to Et and iPr, more charge will be donated to the metal, which will increase the metal contribution to the highest filled orbitals and decrease the metal character of the bonding orbitals. As a result, the intensity of the first absorption band will increase at the expense of that of the second band, as shown in Figure 3.

Figures 2–4 clearly demonstrate the influence of the ligands on the absorption spectra and especially the effect of variation

(41) Balk, R. W.; Stufkens, D. J.; Oskam, A. *Inorg. Chim. Acta* **1979**, *34*, 267.

(42) DeKock, R. L. In *Electron Spectroscopy: Theory, Techniques and Applications;* Brundle, C. R., Baker, A. D., Ed.; Academic Press: London, 1977; Vol. 1, Chapter 6, p 294.

(43) Servaas, P. C.; Stufkens, D. J.; Oskam, A. *Inorg. Chem.* **1989**, *28*, 1774.

of the metal–halide interaction. A similar influence on the absorption spectra has recently been observed for the complexes *fac*-[Mn(X)(CO)₃(α-diimine)] (X = Cl, Br, I). The observed changes were rationalized with the results of MO calculations.

The change of metal–halide interaction not only affects the character of the electronic transitions but also the properties of the lowest-excited states. Preliminary results from emission and excited-state IR studies confirm our assignment.[44,45] Thus, the emission lifetime of the complexes X/Me/iPr-DAB at room temperature increases from 65 to 180 ns going from X = Cl to I,[44] although the emission energy does not change and the spin-orbit coupling even increases. At the same time, the excited state IR spectra show the smallest frequency increase of the CO-stretching vibrations in the case of the iodide complex.[45] Both effects point to a change of character of the lowest excited state from MLCT to XLCT.

(44) Nieuwenhuis, H. A.; Stufkens, D. J.; Vlček, A., Jr. Submitted for publication in *Inorg. Chem.*

(45) Nieuwenhuis, H. A.; Stufkens, D. J.; McGarvey, J. J.; McNicholl, R.; George, M. W.; Westwell, J.; Turner, J. J. To be submitted for publication.

Conclusions

The results discussed in the preceding sections, lead to an interesting conclusion. Although most low-valent transition metal complexes with α-diimines give rise to metal-to-ligand charge transfer transitions in the visible region, the characters of the electronic transitions of [Ru(X)(R)(CO)₂(α-diimine)] strongly depend on the mixing between metal-d_π and halide-p_π orbitals. This mixing results in the formation of new molecular orbitals from which charge transfer transitions to the α-diimine ligand can occur. The composition of these orbitals is also influenced by the electron releasing properties of the alkyl ligand. Obviously, subtle variations of the ligand properties strongly influence the electronic structure of these complexes in their ground and excited states.